Journal of Asian Earth Sciences 73 (2013) 409–418

Contents lists available at SciVerse ScienceDirect

Journal of Asian Earth Sciences

journal homepage: www.elsevier.com/locate/jseaes

Maximum magnitudes in aftershock sequences in Taiwan

Chung-Han Chan *, Yih-Min Wu

Department of Geosciences, National Taiwan University, Taipei, Taiwan

ARTICLE INFO

Article history:
Received 27 November 2012
Received in revised form 16 April 2013
Accepted 3 May 2013
Available online 23 May 2013

Keywords:
Båth's Law
Gutenberg–Richter Law
Modified Omori's Law
Earthquake sequence
Taiwan

ABSTRACT

In this work, Båth's Law, the *b*-value in Gutenberg–Richter Law (G–R Law) in the form of the $1/\beta$ relationship, and both the *a*- and *b*-values in the G–R Law were introduced in order to estimate maximum aftershock magnitudes of earthquake sequences in the Taiwan region. The averaged difference of magnitude between the mainshock and the maximum aftershock is 1.20, and is consistent with Båth's Law, however, with a large uncertainty. The large uncertainty implies that the difference may result from a variable controlled by other factors, such as the aftershocks number of an earthquake sequence and magnitude threshold for mainshock. With $1/\beta$, since 86% of the earthquake sequences with a $M \geqslant 6.0$ mainshock follow this relationship, the upper bound of the maximum magnitude can be estimated for an earthquake sequence with a large mainshock. The *a*- and *b*-values in the G–R Law was also considered by evaluating maximum aftershock magnitudes. As there are low residuals between the model and the observations, the results suggest that the G–R Law is a good index for maximum aftershock magnitude determinations. In order to evaluate the temporal decays of maximum aftershock magnitudes, modified Omori's Law was introduced. Using the approaches mentioned above, the maximum magnitudes and the temporal evolution of an earthquake sequence could be modeled. Among them, the model of the G–R Law has the best fit with observations for most of earthquake sequences. It shows its feasibility. The results of this work may benefit seismic hazards mitigation in the form of rapid re-evaluations for short-term seismic hazards immediately following devastating earthquakes.

1. Introduction

Historical experience has indicated that not only mainshocks, but also subsequent aftershocks may result in seismic hazards. For example, the M_w 6.3, 21 February 2011 Christchurch, New Zealand earthquake is regarded as an aftershock of the M_w 7.1, 4 September 2010 Darfield mainshock (Chan et al., 2012). The Christchurch earthquake caused much more damage and fatalities than the mainshock. Therefore, understanding the behavior of aftershocks, in terms of maximum magnitude and temporal evolution, is a crucial issue for seismic hazards mitigation.

Some of previous studies have investigated maximum magnitudes within earthquake sequences. Båth (1965) concluded that the averaged difference, $\overline{D_1}$, between the magnitudes of the mainshock, M_0, and the largest aftershock, M_1, is, as follows:

$$\overline{D_1} = 1.2 \tag{1}$$

The relationship has been named Båth's Law, and has become one of the most referenced characteristics of earthquake sequences. However, the relationship does not agree with the results of subsequent studies. Utsu (1969) indicated that, instead of a constant, D_1 is a variable that is larger than the expected value $1/\beta$, where β can be represented as follows:

$$\beta = b \cdot \ln(10) \tag{2}$$

where *b* is the *b*-value in Gutenberg–Richter's Law (G–R Law) (Gutenberg and Richter, 1954), as follows:

$$log(N) = a - bM \tag{3}$$

where *N* is the number of events with a magnitude larger than or equal to the magnitude threshold, *M*. Based on aftershock sequences in Japan, Utsu (1961, 1969) obtained a negative correlation between D_1 and M_1, in disagreement with Bath's Law. This hypothesis is confirmed by Lombardi (2002), who analyzed the Southern California catalog and theoretical density function. Besides, based on theoretical density function, Lombardi (2002) found a smaller D_1 for the sequence with a larger aftershock number. Vere-Jones (1969) and Lombardi (2002) further concluded that a larger D_1 is obtained when a larger magnitude difference between magnitude threshold for mainshock and magnitude completeness, M_c, is assumed. Until now, the characteristic of the maximum magnitude in earthquake sequences has remained controversial. To examine the feasibility of each model for maximum aftershock

* Corresponding author. Tel.: +886 2 33664956x309; fax: +886 2 2363 6095.
E-mail address: cchan@ntu.edu.tw (C.-H. Chan).

1367-9120/$ - see front matter © 2013 Published by Elsevier Ltd.
http://dx.doi.org/10.1016/j.jseaes.2013.05.006

determinations using a comparison with observations, a high-quality catalog with a large number of earthquakes is desirable.

Taiwan is located in a region with a high amount of seismic activity and a seismic network of good quality. Due to interactions between the Eurasia and Philippine Sea Plates in Taiwan the seismicity rate is high. The Central Weather Bureau Seismic Network (CWBSN, Fig. 1) has been in operation since early of 1990s. Arrival times of P and S waves are selected manually for earthquake location and Richter local magnitude (M_L) determination in the CWBSN (Shin, 1993). The CWBSN records approximately 20,000 events each year in a region of ca. 400 × 550 km (Wu et al., 2008a). Therefore, in respect to maximum aftershock determinations, Taiwan is a good candidate region for examining the feasibility of each model.

The goal of this work was to determine the characteristics of maximum magnitudes in earthquake sequences in Taiwan. The relationship between M_0 and M_1 is first discussed in order to confirm the feasibility of Båth's Law. M_1 is then estimated according to $1/\beta$, which can be regarded as the lower bound for $\overline{D_1}$. Both the *a*- and *b*-values in the G–R Law are further considered for calculating the maximum aftershock magnitudes. In addition, the temporal evolutions of the maximum aftershocks are also discussed. Four earthquake sequences are introduced and the feasibility of each model is examined using a comparison with observations.

2. The earthquake catalog and the clustering methodology

Events with a magnitude larger than the magnitude of completeness, M_c, in the CWBSN catalog were considered for the analysis. A clustering method was used for extracting earthquake sequences. In the following, the spatial distribution of M_c and the clustering methodology are introduced.

2.1. The spatial distribution of M_c

The CWBSN, since the early 1990s, has greatly enhanced the capability of earthquake monitoring (Wu and Chiao, 2006). To evaluate the reliability of the catalog, we calculated the spatial distribution of M_c by using the maximum curvature approach (Wiemer and Wyss, 2000). We considered the catalog over the period between 1993 and 2011 for shallow earthquakes (with a focal depth $\leqslant$ 30 km), divided our study region into 0.2° × 0.2° grids, and searched for events that occurred in a circle with a radius of 30 km (Fig. 1). The pattern of M_c simply reflects the density of

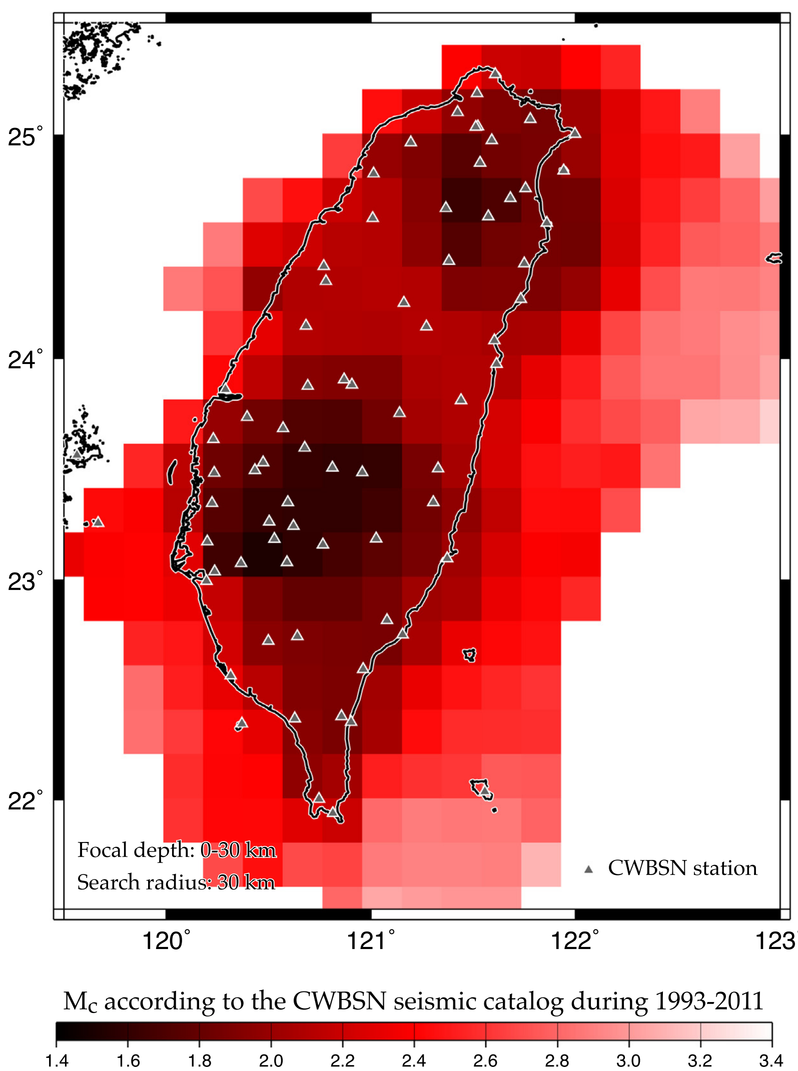

Fig. 1. The spatial distribution of the magnitude completeness (M_c) for the Central Weather Bureau Seismic Network (CWBSN) catalog. Triangles represent the locations of the CWBSN stations.

the seismic stations (triangles in Fig. 1). The number of stations is highest in northern and southwestern Taiwan, where the M_c is as low as 1.5. The M_c for the inland region is generally less than 2.0, whereas in offshore regions, due to poor network coverage, it is between 2.5 and 3.2. The spatial distribution and the magnitudes estimated in this study are consistent with those obtained from the Bayesian magnitude of completeness method (Mignan et al., 2011). To fulfill the same criteria for our calculations, we re-evaluated M_c according to the catalog.

2.2. Clustering methodology

To extract earthquake clusters for events that are related to one another in the catalog, the spatiotemporal double-link cluster analysis was applied (Wu and Chiao, 2006). The approach is modified from the single-link cluster analysis by Davis and Frohlich (1991). Events within the spatial and temporal windows of mainshock will be identified as aftershocks. Other events within the spatial and temporal windows of identified aftershocks will also be identified as aftershocks. Repeating such process for many times can identify the most of the aftershocks in a wide area and longer period. We set spatial and temporal linking parameters of 5 km and 3 days, respectively, as commonly used for earthquake clustering in Taiwan (Wu and Chiao, 2006; Wu and Chen, 2007; Wu et al., 2008b). Following the clustering approach, a total of 706 earthquake sequences are selected for the analysis (Fig. 2).

3. What factors control the maximum magnitude within a sequence?

Considering the studied earthquake sequences (Fig. 2), the largest aftershock, M_1, of each sequence is observed (the horizontal component in Fig. 3a). The range of the corresponding M_1 is between 0.0 (no consequent event) and 6.8 (the aftershock of the 1999 Chi-Chi earthquake). In the following, we attempt to fit the observations with the models mentioned above in order to understand their behavior.

3.1. Båth's Law

According to Båth's Law, represented by equation (2), the difference, D_1, between M_0 and M_1 is a constant. In order to test the feasibility of this law, the D_1 of each sequence was evaluated (Fig. 3). We first considered all of the sequences (all stars in Fig. 2). The $\overline{D_1}$ of 1.20 is determined (Fig. 3a), corresponding to the conclusions of Båth (1965). The standard deviation is obtained according to the comparison between magnitude of mainshocks minus 1.20 ($\overline{D_1}$) and magnitudes of maximum aftershocks. The corresponding standard deviation is 0.73 (dashed lines in Fig. 3a). The relative high standard deviation implies that some of the sequences may depart from Båth's Law. We found that most of sequences with large $\overline{D_1}$ have small number of events. Among the 93 sequences with $\overline{D_1}$ above the standard deviation, 51 of them (55%) have a number of

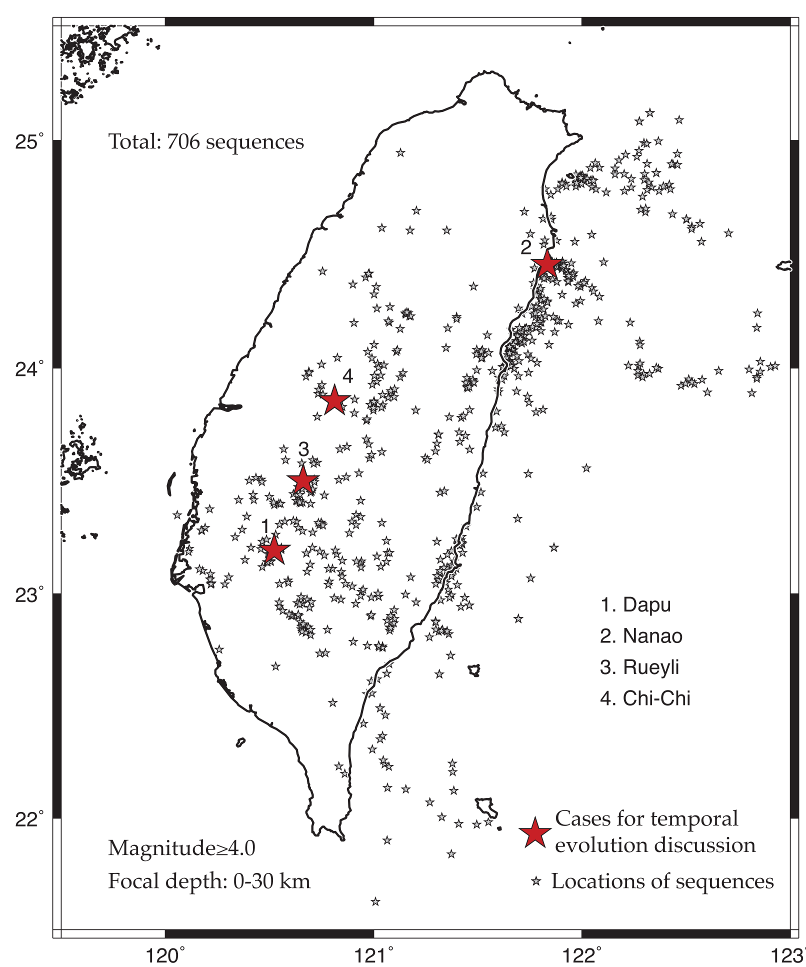

Fig. 2. The distribution of the 706 investigated sequences in Taiwan, selected by a spatiotemporal double-link cluster analysis. Earthquakes with a M_L greater than or equal to 4.0 and focal depths less than 30 km from 1993 to 2011are selected. Large stars represent the sequences used for the discussion of temporal evolution.

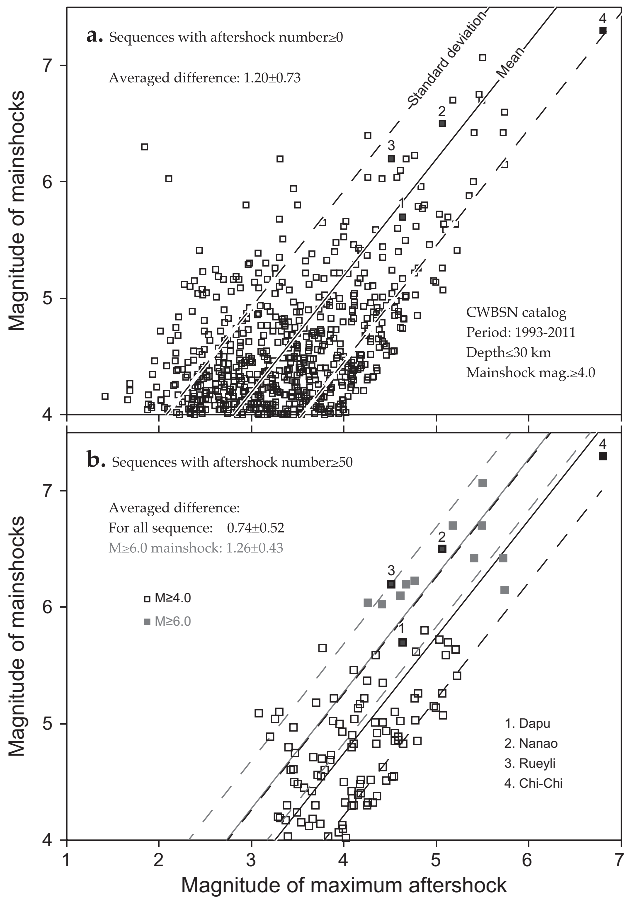

Fig. 3. A comparison between the magnitude of the mainshock and that of the maximum aftershock (a) for each sequence and (b) for the sequence with aftershocks number larger or equal to 50. The data for the sequences with $M \geqslant 6.0$ mainshock are presented in gray squares. The average difference between each with a standard deviation are denoted as solid and dashed lines, respectively. The data for the Dapu, Nanao, Rueyli, and Chi-Chi sequences are denoted as solid black squares.

events smaller or equal to 5, and 74 of them (80%) have a number of events smaller or equal to 10. In order to further confirm the relationship between event number and $\overline{D_1}$, only the earthquake sequences with an aftershocks number larger than 50 were considered (Fig. 3b). A lower $\overline{D_1}$ (0.74) with a relative smaller standard deviation (0.52) is determined (Fig. 3b). $\overline{D_1}$ for the sequences with a $M \geqslant 6.0$ mainshock (gray squares in Fig. 3b) were further evaluated. The $\overline{D_1}$ of 1.26 with standard deviation of 0.43 is determined.

3.2. The *b*-value

Based on the statement of Utsu (1969), D_1 is larger than the expected value $1/\beta$. In order to examine the hypothesis, the $1/\beta$ for each earthquake sequence was evaluated (Fig. 4). A maximum likelihood estimation is used to calculate the *b*-value. In consideration the reliability in calculating *b*-values, earthquake sequences with aftershocks number larger than 50 are analyzed. This number corresponds to a relative small standard deviation, σ, of 0.14 when *b*-value equal to 1.0 according to the relation (Aki, 1965):

$$\sigma = bN^{-1/2} \tag{4}$$

Considering this qualification, there are 119 sequences for the analysis. Fifty-six percent (67 of 119) of the sequences have a

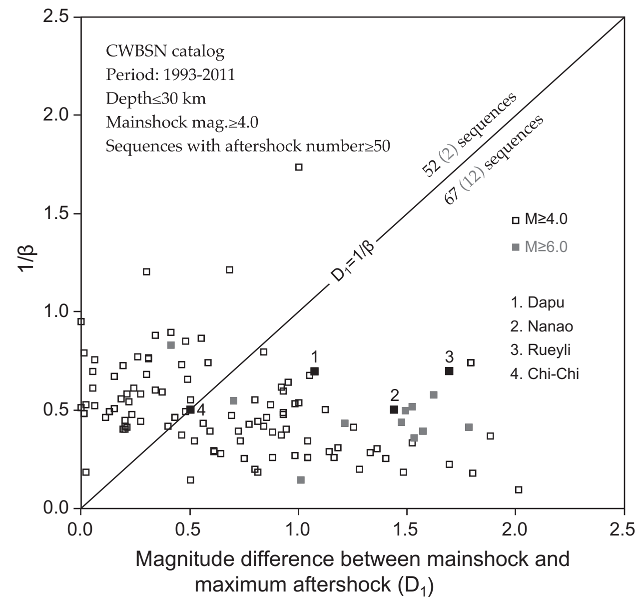

Fig. 4. The comparison between the $1/\beta$ and the magnitude difference between the mainshock and the observed maximum aftershock (D_1) in sequences with numbers of aftershocks larger than 50. The data for the Dapu, Nanao, Rueyli, and Chi-Chi sequences are denoted as solid black squares.

lower $1/\beta$ in comparison to D_1. When only the sequences with a $M \geqslant 6.0$ mainshock (gray squares in Fig. 4) were considered, 86% (12 of 14) of the sequences have a lower $1/\beta$. The results might imply that only the sequences with large mainshock correspond to the conclusion of Utsu (1969).

3.3. The G–R Law

In addition to the *b*-value, the *a*-value in the G–R Law (Eq. (3)) was also introduced in order to determine the maximum aftershock magnitude. It was assumed that M_1 is obtained when *N*

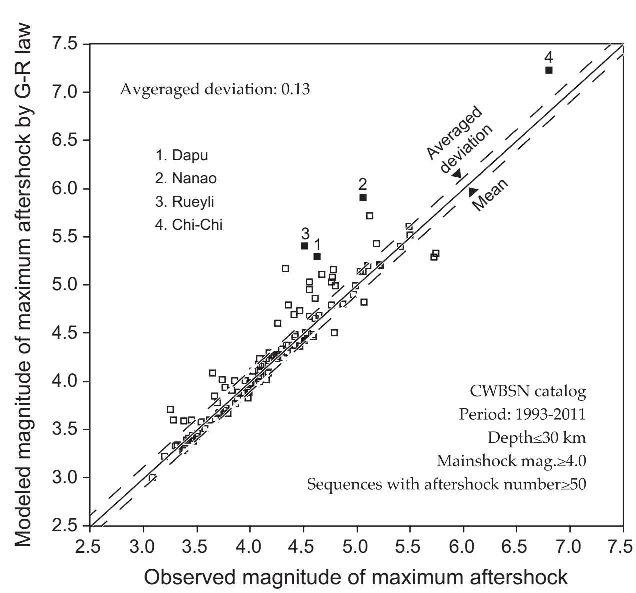

Fig. 5. The comparison between the observed and modeled magnitudes of the maximum aftershocks in a sequence with the number of aftershocks larger than 50. The models were based on the G–R Law. The averaged deviation between the observations and the models for the 119 sequences was 0.13. The data for the Dapu, Nanao, Rueyli, and Chi-Chi sequences are denoted as solid black squares.

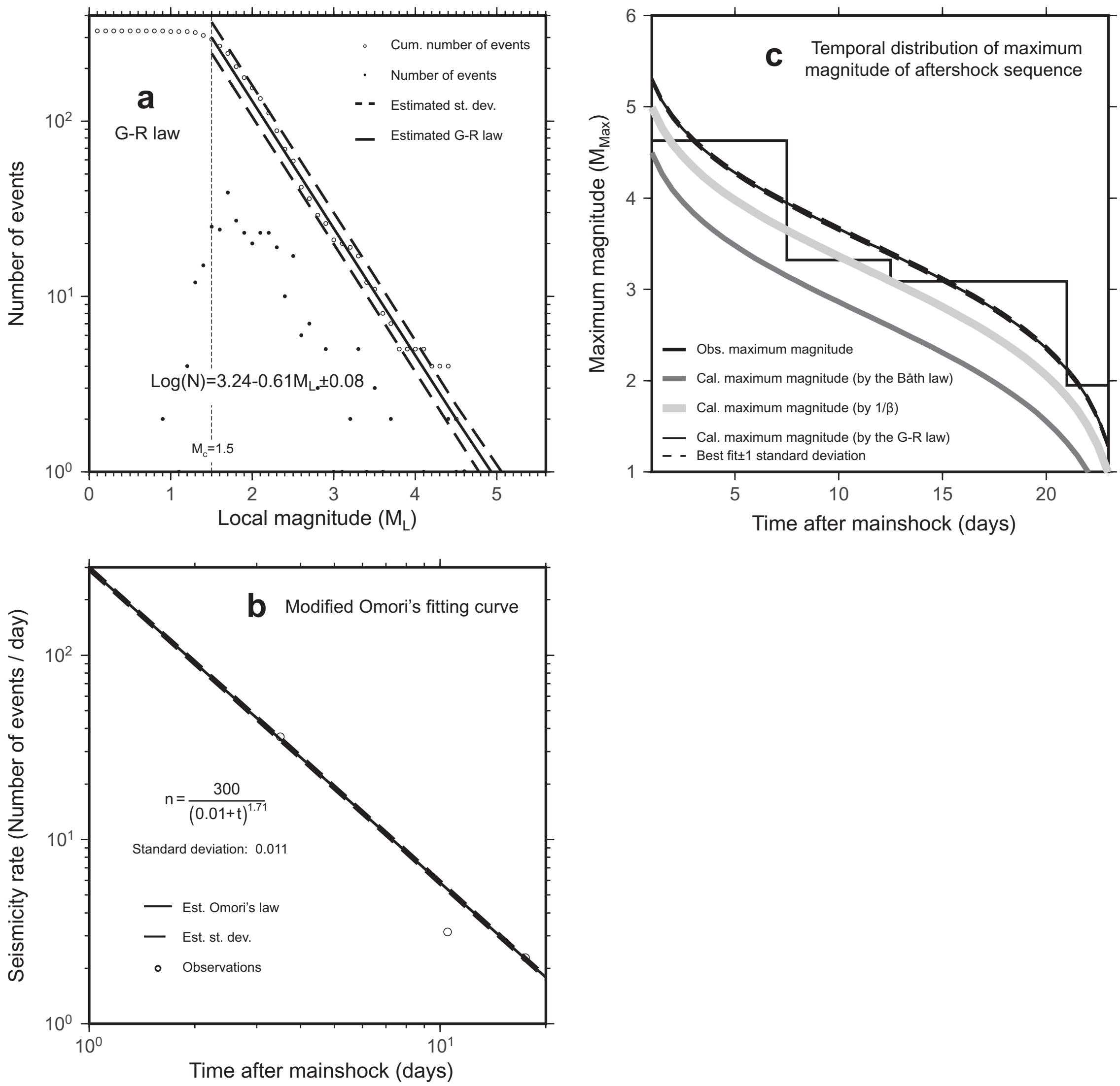

Fig. 6. (a) The modeled G–R Law, (b) the modeled modified Omori's Law, and (c) the observed and modeled temporal distribution of the maximum magnitude of the 1993 Dapu sequence. The residuals for the temporal evolution based on these three approaches are presented in Table 1.

is equal to 1 (i.e. $M_1 = \frac{a}{b}$). To compare the modeled M_1 with the observed one for each sequence (Fig. 5), the consistency between each is confirmed by the relatively low averaged deviation of 0.13.

4. Case studies for modeling the temporal evolution of aftershock magnitudes

The approaches outlined above have been proposed for modeling maximum magnitudes in sequences. In the following we evaluate the temporal distribution in a sequence. For estimating the seismicity rate, $n(t)$, that decays with time, t, we considered the modified Omori's Law of Utsu (1961) and Utsu et al. (1995), which can be denoted as follows:

$$n(t) = \frac{k}{(c+t)^p} \tag{5}$$

where k, c, and p are constants. In this study, the three parameters for each sequence were obtained using a best fit with the observations. The total number of aftershocks, N_1, following time t_1 are presented, as follows:

$$N_1 = \int_{t_1}^{t_{end}} \frac{k}{(c+t)^p dt}, \tag{6}$$

where t_{end} is the time for the end of sequence. We evaluated the ratio of N_1 to N for various periods then modeled the decay of maximum aftershocks magnitudes by assuming a variable a-value and a fixed b-value for the G–R Law. We modeled the temporal evolution of aftershock magnitudes for the 1993 Dapu, 1994 Nanao, 1998 Rueyli, and 1999 Chi-Chi earthquake sequences (Chan and Ma, 2004).

4.1. The 1993 Dapu earthquake sequence

To model the spatial and temporal distribution of the 1993 Dapu sequence, the G–R Law (Fig. 6a) and modified Omori's Law (Fig. 6b) were introduced. Based on the magnitude of the mainshock (M_L = 5.7) and Båth's Law, that D_1 = 1.2, M_1 is expected to be 4.5. Based on the b-value of 0.61 (Fig. 6a) and the $1/\beta$ relationship, M_1 is expected to be smaller than 5.0. According to the modeled a- and b-values in the G–R Law are 3.24 and 0.61, respectively. The M_1 is expected to be 5.3 (Table 1). As comparison to the observed M_1 (4.6), the Båth's Law relationship performs best.

Table 1
The source parameters for the mainshocks of the four sequences that were considered for the discussion of the temporal evolutions of aftershock magnitudes. The observed and modeled M_1, as well as the residual for temporal evolution based on the three approaches, are presented.

Earthquake	Dapu	Nanao	Rueyli	Chi-Chi
Origin time				
Year	1993	1994	1998	1999
Month	12	6	7	9
Day	15	5	17	20
Hour	21	1	4	17
Minute	49	9	51	47
Second	43.10	30.09	14.96	15.85
Location				
Longitude (°)	120.52	121.83	120.66	120.81
Latitude (°)	23.19	24.46	23.50	23.86
Depth (km)	12.5	5.3	2.8	8.0
Mainshock magnitude (M_L)	5.7	6.5	6.2	7.3
Max. magnitude				
Observation	4.6	5.1	4.5	6.8
Båth	4.5 (−0.1)	5.3 (+0.2)	5.0 (+0.5)	6.1 (−0.7)
$1/\beta$	5.0 (+0.4)	6.0 (+0.9)	5.5 (+1.0)	6.8 (0.0)
G–R	5.3 (+0.7)	5.9 (+0.8)	5.4 (+0.9)	7.3 (+0.5)
Residual for temporal evolution				
Båth	0.87	0.55	0.47	0.45
$1/\beta$	0.44	0.36	0.54	0.39
G–R	0.35	0.32	0.41	0.76

According to the date of the last event in the Dapu sequence (8 January 1994), t_{end} is 24 days. Based on the modeled modified Omori's Law (Fig. 6b), N_1 can be evaluated as a function of t_1 according to equation (6). By assuming a variable a-value and a fixed b-value, the temporal decay of M_1 can be evaluated. For example, when $t_1 = 4.9$ days, N_1 becomes 1/4.07 times the value from the beginning of the sequence. The a-value becomes 3.24-log (4.07) = 2.63. Considering the b-value of 0.61, the M_1 for this moment will be 1 unit smaller than when it was in the beginning. Based on this procedure, the temporal evolution for M_1 can be modeled, using Båth's Law, $1/\beta$, or the modeled a- and b-values in the G–R Law, (Fig. 6c). As compared with the observation (the thinnest line in Fig. 6c) that represents M_1 for each time point until the end of the sequence, all three of the approaches can model the trend of decay.

4.2. The 1994 Nanao earthquake sequence

For the 1994 Nanao earthquake sequence, based on the magnitude of the mainshock ($M_L = 6.5$) and Båth's Law, M_1 is expected to be 5.3; based on the b-value of 0.84 and the $1/\beta$ relationship, M_1 is expected to be smaller than 6.0; and based on the modeled a- and b-values (3.24 and 0.61, respectively) in the G–R Law, M_1 is expected to be 5.9 (Table 1). As comparison to the observed M_1 (5.1), Båth's Law relationship performs best.

According to the date of the last event in the Dapu sequence (31 August 1995), t_{end} is 87 days. Based on the modeled modified Omori's Law (Fig. 7b), the temporal evolution for the magnitudes of maximum aftershocks can be modeled according to those approaches mentioned above (Fig. 6c).

4.3. The 1998 Rueyli earthquake sequence

For the 1998 Rueyli earthquake sequence, based on the magnitude of the mainshock ($M_L = 6.2$) and Båth's Law, M_1 is expected to be 5.0; based on the b-value of 0.65 and the $1/\beta$ relationship, M_1 is expected to be smaller than 5.5; and since the modeled a- and b-values in the G–R Law are 3.49 and 0.65, respectively, M_1 is expected to be 5.4 (Table 1). As comparison to the observed M_1 (4.5), Båth's Law relationship performs best.

According to the date of the last event in the Rueyli sequence (13 August 1998), t_{end} is 27 days. Based on the modeled modified Omori's Law (Fig. 8b), the temporal evolution for the magnitudes of maximum aftershocks can be modeled according to those three approaches (Fig. 6c).

4.4. The 1999 Chi-Chi earthquake sequence

For the 1999 Chi-Chi earthquake sequence, based on the magnitude of the mainshock ($M_L = 7.3$) and Båth's Law, M_1 is expected to be 6.1; based on the b-value of 0.85 and the $1/\beta$ relationship, M_1 is expected to be smaller than 6.8; and based on the modeled a- and b-values in the G–R Law are 6.26 and 0.85, respectively, M_1 is expected to be 7.3 (Table 1). As comparison to the observed M_1 (6.8), the $1/\beta$ relationship performs best.

According to the date of the last event in the Chi-Chi sequence (5 May 2000), t_{end} is 151 days. Based on the modeled modified Omori's Law (Fig. 9b), the temporal evolution for the magnitudes of maximum aftershocks can be modeled according to those three approaches (Fig. 9c).

4.5. Summary of the four cases

We compared the observed maximum aftershock magnitudes with modeled ones using different approaches and found that Båth's Law relationship performs best in the Dapu, Nanao, and Rueyli sequences. In the Chi-Chi case, modeled M_1 based on the $1/\beta$ relationship fits the observed one best. Note that based on the statement of Utsu (1969), D_1 is larger than the expected value $1/\beta$. Thus all of the four sequences obey this statement.

The temporal evolution for the magnitudes of maximum aftershocks are modeled and compared with the observations for the four sequences (Figs. 6c, 7c, 8c, and 9c). We compared the observations and the models and reported the averaged residuals (Table 1). The models of the G–R Law has the best fitting with observations in the Dapu, Nanao, and Rueyli sequences. In the Chi-Chi case, the $1/\beta$ relationship presents least averaged residual. It has the best performance.

5. Discussion and summary

5.1. The feasibility of the models for determining maximum magnitude in a sequence

In this study, Båth's Law, the $1/\beta$ relationship, and the G–R Law were introduced in order to model the maximum magnitude of earthquake sequences in Taiwan. All of the approaches demonstrated their feasibility within the range of uncertainty. The $\overline{D_1}$ is 1.20 when all of the earthquake sequences are considered (Fig. 3a). It is consistent with the conclusion of Båth (1965). However, a large deviation of 0.73 implies that the difference may result from a variable. In other words, D_1 is also controlled by other factors, such as number of aftershocks (Lombardi, 2002), the magnitude threshold for mainshock (Vere-Jones, 1969; Lombardi, 2002), and/or b-value in the G–R Law (Utsu, 1969; Lombardi, 2002).

We also clarify the factors that control D_1. A relatively lower $\overline{D_1}$ of 0.74 is determined when the earthquake sequences with an aftershocks number larger than 50 are analyzed (Fig. 3b). Such result suggests a larger aftershocks number leads to a smaller D_1. It corresponds to the conclusions of Lombardi (2002). The factor of different thresholds for mainshocks is also discussed. When the

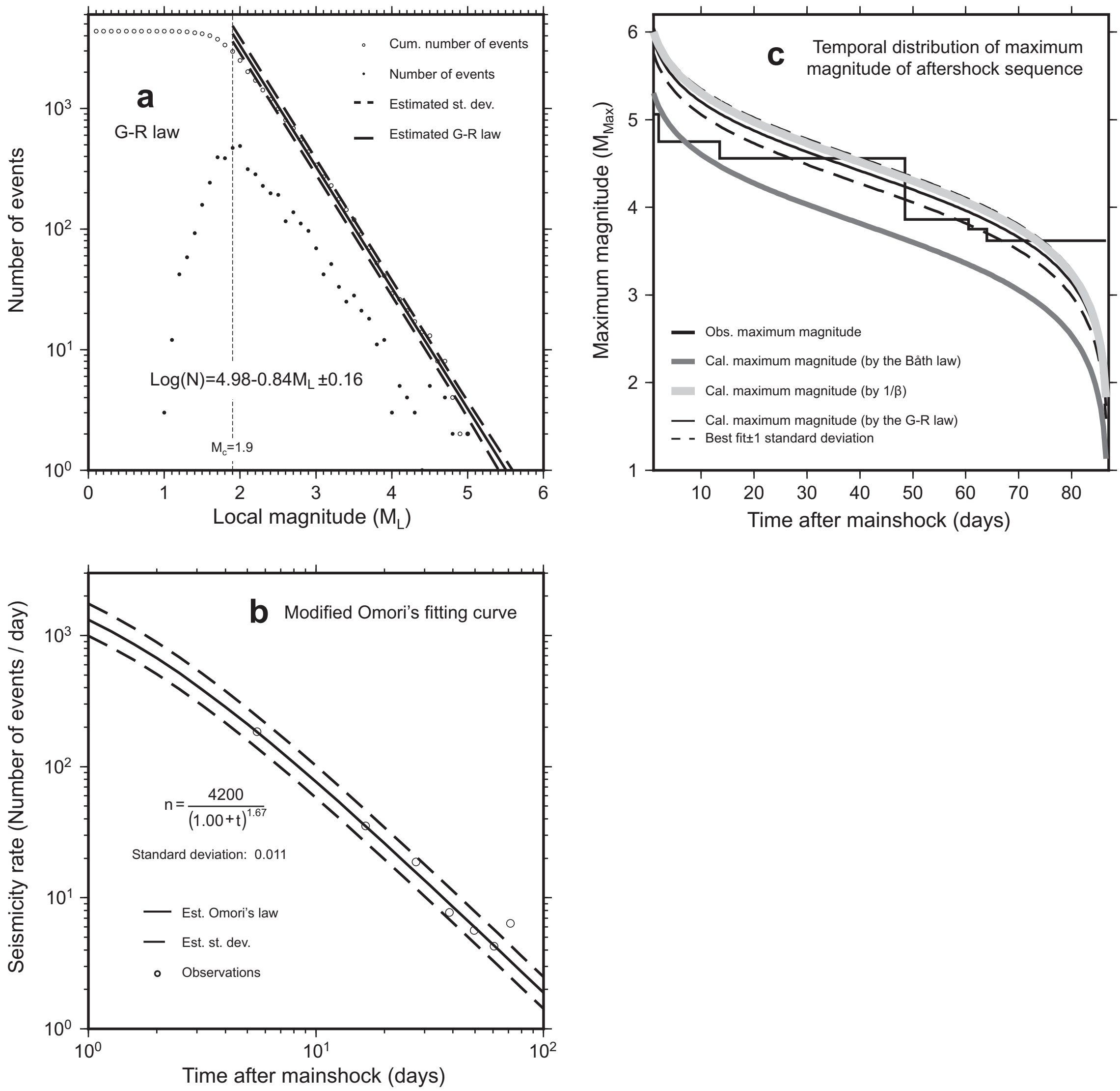

Fig. 7. (a) The modeled G–R Law, (b) the modeled modified Omori's Law, and (c) the observed and modeled temporal distribution of the maximum magnitude of the 1994 Nanao sequence. The residuals for the temporal evolution based on these three approaches are presented in Table 1.

sequences with a $M \geqslant 6.0$ mainshock are analyzed (the gray squares in Fig. 3b), the $\overline{D_1}$ of 1.26 is obtained. It represents a significant higher D_1 in comparison with result from those of the sequences with a $M \geqslant 4.0$ mainshock (all squares in Fig. 3b). This result suggests that a larger difference between magnitude threshold for mainshock and M_c brings a higher D_1. It corresponds to the conclusions of Lombardi (2002) and Vere-Jones (1969).

The correlation between D_1 and the b-value in the form of the $1/\beta$ relationship is also discussed (Fig. 4). It shows only 56% of the sequences has a larger D_1 than$1/\beta$. It does not fully agree with the statement of Utsu (1969). However, when the sequences with a $M \geqslant 6.0$ mainshock (gray squares in Fig. 4) are analyzed, 86% of them follow the statement. These results might be attributed to the following two reasons: (1) only the sequences with large mainshocks follow this relationship; or (2) according to the conclusions of Lombardi (2002) and Vere-Jones (1969), a larger difference between magnitude threshold for mainshock and M_c results in a higher D_1.

The G–R Law also provides an evaluation for the maximum aftershock magnitude (Fig. 5). According to the low deviation of 0.13 between the models and the observations, the G–R Law can be an ideal index for maximum aftershock magnitude determinations.

5.2. The temporal evolution of maximum magnitude in earthquake sequences

The modified Omori's Law is applied in order to model the temporal evolution of seismicity rate in an earthquake sequence. Considering maximum aftershocks through Båth's Law, the $1/\beta$ relationship, or the modeled a- and b-values in the G–R Law, the maximum aftershock magnitude as function of time can be evaluated. To test the feasibility, we applied to the 1993 Dapu (Fig. 6), 1994 Nanao (Fig. 7), 1998 Rueyli (Fig. 8), and 1999 Chi-Chi (Fig. 9) earthquake sequences, respectively. The model of the G–R Law has the best fitting with observations for three of the four sequences (Table 1). It shows its feasibility.

5.3. The difficulty of modeling the occurrence of consequent large earthquakes

In this study, we evaluated possible maximum magnitudes in aftershock sequences. We assumed consequent earthquakes are smaller than the first event in a sequence. However, the consequent earthquakes sometimes are larger than the first one. For example, on 9 March 2011 a M_w 7.4 earthquake took place in the

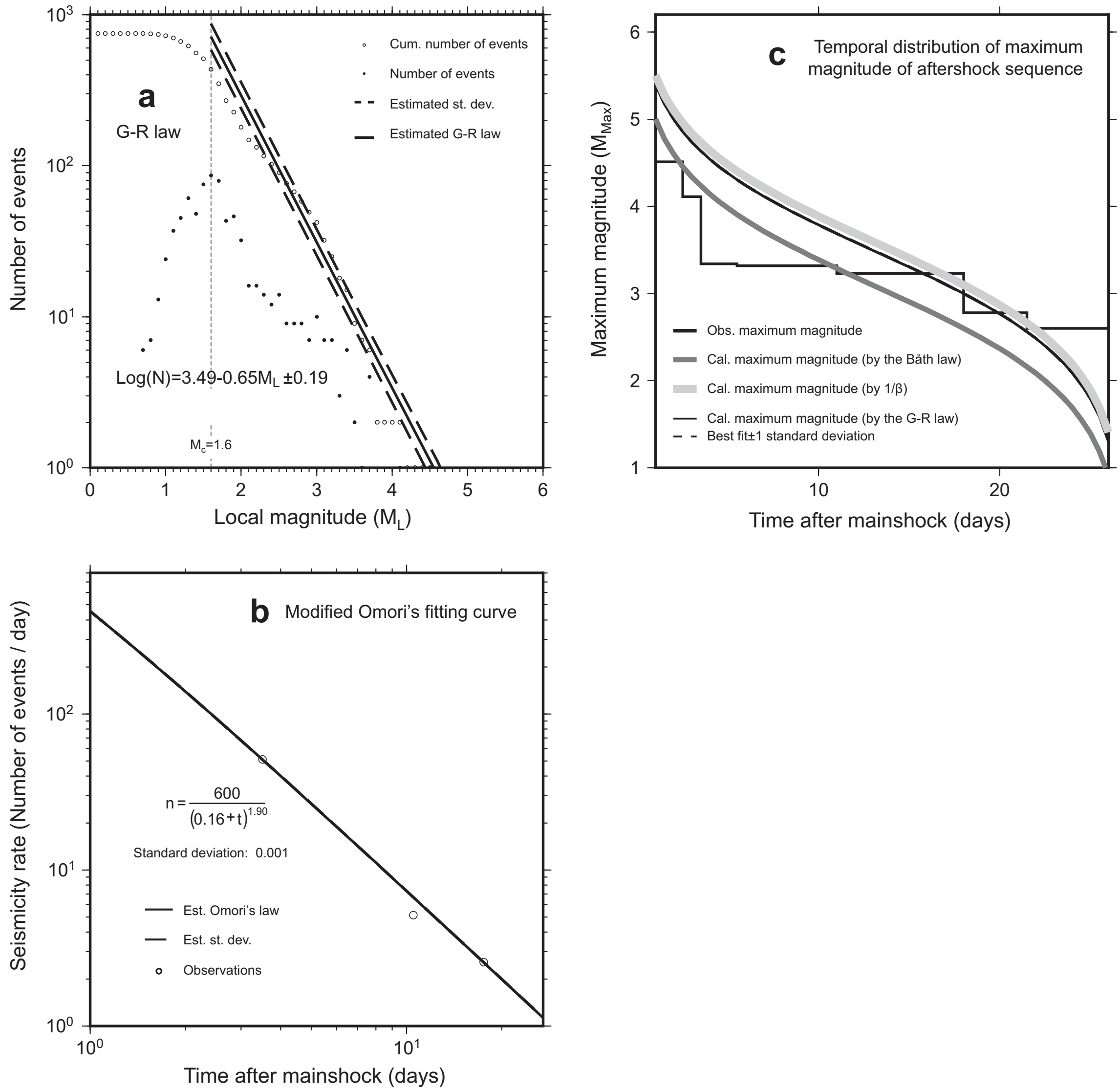

Fig. 8. (a) The modeled G–R Law, (b) the modeled modified Omori's Law, and (c) the observed and modeled temporal distribution of the maximum magnitude of the 1998Rueyli sequence. The residuals for the temporal evolution based on these three approaches are presented in Table 1.

offshore region of the Pacific coast of Tohoku, Japan (Nettles et al., 2011). Since the epicenter was away from land, the resulting damage was negligible. However, 51 h later, on March 11th, a giant earthquake with a M_w 9.1 took place and resulted in disasters in Japan. Thus, it is desired to evaluate possibility of the next larger earthquakes in an earthquake sequence for seismic hazard mitigation.

However, all three of the approaches are less user-friendly for evaluating the probability of consequent earthquakes with larger magnitudes (i.e. when the first earthquake becomes a foreshock). Based on the approaches of Båth's Law and the $1/\beta$ relationship, the maximum magnitude in a sequence is assumed to be smaller than the magnitude of the first event. Based on the G–R Law, the modeled magnitude of a sequence could be larger than that of the mainshock when a large *a*-value and/or a small *b*-value are obtained. Alternatively, foreshock–mainshock behaviors can be modeled in the form of physics-based or statistics-based approaches. For example, Chan et al. (2010, 2012), Chan and Wu (2012) considered the Coulomb stress change imparted by earthquakes and the rate-and-state friction model in order to evaluate the seismicity rate evolution. Based on this approach, the occurrence probabilities for different magnitudes can be estimated. Additionally, the Time–space Epidemic Type AfterShock model (known as the ETAS model by Kagan and Knopoff, 1978) is an alternative. Based on this model, every earthquake is assumed to be a mainshock that can trigger subsequent events that could be larger than the mainshock.

5.4. A possible application in near real-time

Based on the approaches proposed in this study, the maximum aftershock magnitudes and their temporal evolutions can be modeled. The obtained results may be of benefit to decision-makers for seismic hazards mitigation. For example, a rapid evaluation for the short-term seismic hazards immediately following devastating earthquakes could provide information on devastation estimations, emergency response, and/or victim sheltering. Therefore, an approach that can be applied in real-time or near real-time following the occurrence of a large earthquake is desirable. Since it assumes a constant magnitude difference between the mainshock and the maximum aftershock, Båth's Law could be applied immediately following an earthquake. The $1/\beta$ relationship may also be applied in real-time based on the assumption of a temporal-stationary

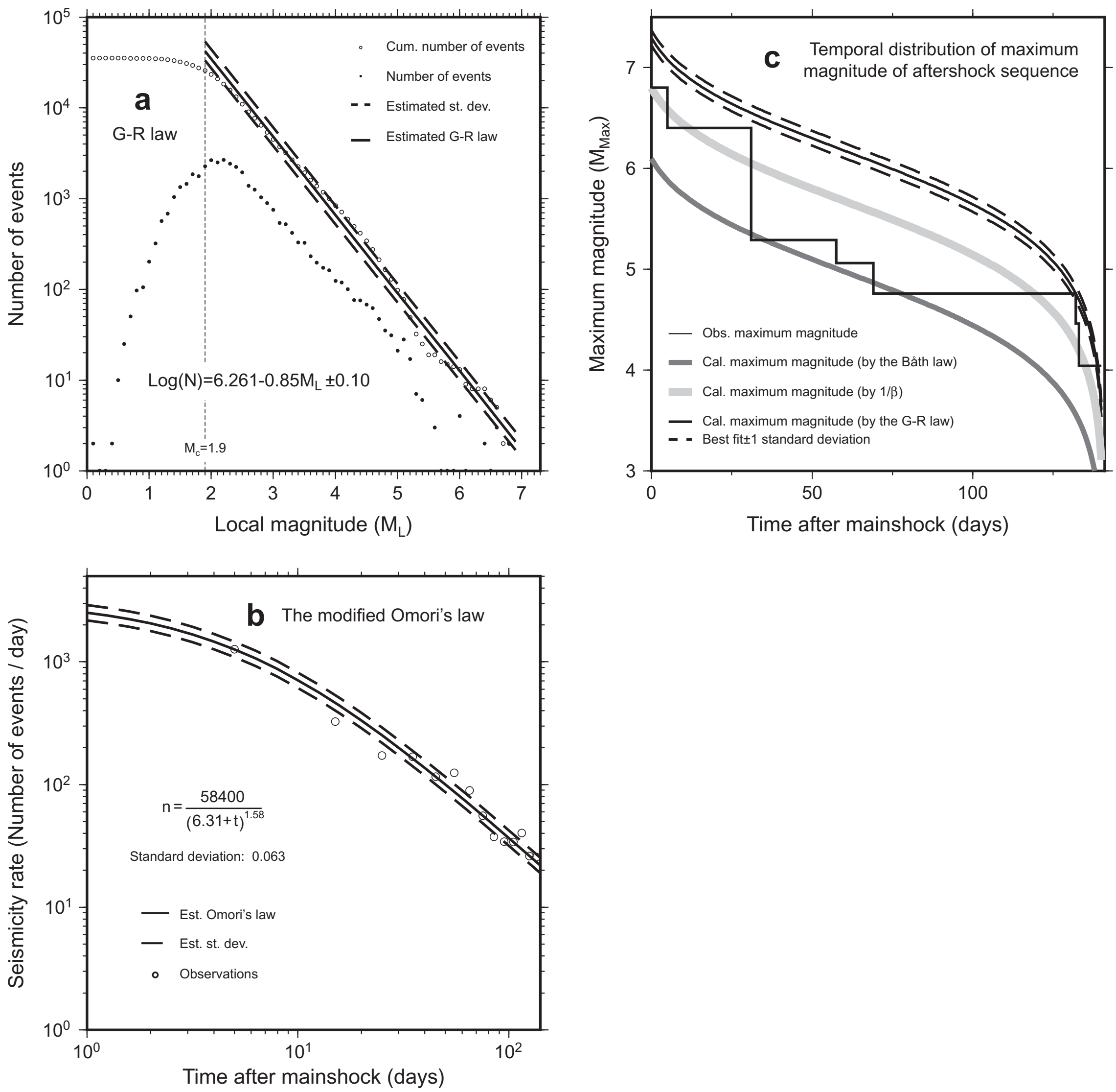

Fig. 9. (a) The modeled G–R Law, (b) the modeled modified Omori's Law, and (c) the observed and modeled temporal distribution of the maximum magnitude of the 1999 Chi-Chi sequence. The residuals for the temporal evolution based on these three approaches are presented in Table 1.

b-value. In practice, once a database for the spatial distribution of *b*-values has been established, the corresponding magnitude of the maximum aftershock can be obtained immediately following the occurrence of the mainshock.

Acknowledgements

Our work was supported by the Central Weather Bureau and the National Science Council, Taiwan.

References

Aki, K., 1965. Maximum likelihood estimate of b in the formula $\log N = a\text{-}bM$ and its confidence. Bull. Earthquake Res. Inst. Univ. Tokyo 43, 237–239.
Båth, M., 1965. Lateral inhomogeneities of the upper mantle. Tectonophysics 2, 483–514.
Chan, C.H., Ma, K.F., 2004. Association of five moderate-large earthquakes to the faults in Taiwan. Terr., Atmosp. Oceanic Sci. 15 (1), 97–110.
Chan, C.H., Wu, Y.M., 2012. The burst of seismicity after the 2010 M6.4 Jiashian earthquake and its implication of short-term seismic hazard in southern Taiwan. J. Asian Earth Sci. 59, 231–239.
Chan, C.H., Sørensen, M.B., Stromeyer, D., Grünthal, G., Heidbach, O., Hakimhashemi, A., Catalli, F., 2010. Forecasting Italian seismicity through a spatio-temporal physical model: importance of considering time dependency and reliability of the forecast. Ann. Geophys. 53 (3). http://dx.doi.org/10.4401/ag-4761.
Chan, C.H., Wu, Y.M., Wang, J.P., 2012. Earthquake forecasting through a smoothing Kernel and the rate-and-state friction law: application to the Taiwan region. Natural Hazards Earth Syst. Sci. 12, 1–13. http://dx.doi.org/10.5194/nhess-12-1-2012.
Davis, S.D., Frohlich, C., 1991. Single-link cluster analysis of earthquake aftershocks: decay laws and regional variations. J. Geophys. Res. 96, 6336–6350.
Gutenberg, B., Richter, C., 1954. Seismicity of the Earth and Associated Phenomena, second ed. Princeton University Press, Princeton, NJ.
Kagan, Y., Knopoff, L., 1978. Statistical study of the occurrence of shallow earthquakes. Geophys. J. Roy. Astron. Soc. 55, 67–86.
Lombardi, A.M., 2002. Probabilistic interpretation of Bath's law. Ann. Geophys. 45, 455–472.
Mignan, A., Werner, M.J., Wiemer, S., Chen, C.C., Wu, Y.M., 2011. Bayesian estimation of the spatially varying completeness magnitude of earthquake catalogs. Bull. Seismol. Soc. Am. 101, 1371–1385. http://dx.doi.org/10.1785/0120100223.
Nettles, M., Ekstroem, G., Koss, H.C., 2011. Centroid-moment-tensor analysis of the 2011 off the Pacific coast of Tohoku Earthquake and its larger foreshocks and aftershocks. Earth Planets Space 63, 519–523.
Shin, T.C., 1993. The calculation of local magnitude from the simulated Wood-Anderson seismograms of the short-period seismograms. Terr., Atmosp. Oceanic Sci. 4, 155–170.
Utsu, T., 1961. A statistical study of the occurrence of aftershocks. Geophys. Mag. 30, 521–605.
Utsu, T., 1969. Aftershock and earthquakes statistics (I). J. Faculty Sci., Hokkaido Univ. 3, 129–195.

Utsu, T., Ogata, Y., Matsu'ura, R.S., 1995. The centenary of the Omori formula for a decay law of aftershock activity. J. Phys. Earth 43, 1–33.
Vere-Jones, D., 1969. A note on the statistical interpretation of Bath 's Law. Bull. Seismol. Soc. Am. 59, 1535–1541.
Wiemer, S., Wyss, M., 2000. Minimum magnitude of completeness in earthquake catalogs: examples from Alaska, the Western United States, and Japan. Bull. Seismol. Soc. Am. 90 (4), 859–869.
Wu, Y.M., Chen, C.C., 2007. Seismic reversal pattern for the 1999 Chi-Chi, Taiwan, Mw7.6 earthquake. Tectonophysics 429, 125–132.
Wu, Y.M., Chiao, L.Y., 2006. Seismic quiescence before the 1999 Chi-Chi, Taiwan Mw7.6 earthquake. Bull. Seismol. Soc. Am. 96, 321–327.
Wu, Y.M., Chang, C.H., Zhao, L., Teng, T.L., Nakamura, M., 2008a. A comprehensive relocation of earthquakes in Taiwan from 1991 to 2005. Bull. Seismol. Soc. Am. 98, 1471–1481. http://dx.doi.org/10.1785/0120070166.
Wu, Y.M., Chen, C.C., Zhao, L., Chang, C.H., 2008b. Seismicity characteristics before the 2003 Chengkung, Taiwan earthquake. Tectonophysics 457, 177–182. http://dx.doi.org/10.1016/j.tecto.2008.06.007.